Low Temperature Physics/Fizika Nizkikh Temperatur, 2021, vol. 47, No. 1, pp. 5–10

Thermo emf in a two-dimensional electron-hole system in HgTe quantum wells in the presence of magnetic field. The role of the diffusive and the phonon-drag contributions

E. B. Olshanetsky[1], Z. D. Kvon[1,2], G. M. Gusev[3], M. V. Entin[1], L. I. Magarill[1], and N. N. Mikhailov[1]

[1]*Institute of Semiconductor Physics, Novosibirsk 630090, Russia*
E-mail: kvon@thermo.isp.nsc.ru

[2]*Novosibirsk State University, Novosibirsk 630090, Russia*

[3]*Instituto de Fsica da Universidade de São Paulo, São Paulo 135960-170, SP, Brazil*

Received September 09, 2020, published online November 24, 2020

We present an experimental study of the thermo emf of a two-dimensional electron-hole system in a 21 nm HgTe quantum well in the presence of magnetic field. The first experimental observation of Nernst–Ettingshausen effect in a 2D semimetal is reported. The comparison between theory and experiment shows that the thermo emf is determined by two contributions: the diffusion and the phonon drag, with the latter contribution several times greater than the first. The conclusion is drawn about the important role of electron-hole scattering in the formation of both thermoelectric power mechanisms.

Keywords: quantum well, 2D semimetal, diffusion, phonon drag.

1. Introduction

The CdHgTe/HgTe/CdHgTe quantum well (QW) has been recently found to go through a rich variety of physically distinct states or phases, depending on the width of the HgTe layer [1, 2]. Below ($d \le 6.3$ nm) the layer is a normal 2D band insulator. At the critical width $d \approx 6.3$ nm the layer becomes a 2D Dirac fermion system with a gapless linear spectrum in the vicinity of Dirac point. Then, on increasing the width above the critical value, the layer evolves into a 2D topological insulator with inverted bulk bands and gapless 1D Dirac states circulating along the sample perimeter. On further increasing the width the layer spectrum remains inverted, although, depending on the width, both the conduction and valence bands may be formed by higher index 2D subbands originating from the 3D HgTe heavy hole band. At the layer width of about 13–14 nm the lateral maximum of the HH2 valence band grows higher than the HH1 conductance band minimum in the centre of the Brillouin zone and the system becomes an indirect 2D semimetal, [3]: both the 2D electron and 2D hole degenerate Fermi gases may be simultaneously present in the system. Note, that in the bulk energy gap between the central conductance band minimum and the $k = 0$ valence band maximum the 1D Dirac edge states are still present.

The coexistence of two distinct carrier types of opposite sign in a 2D semimetal in HgTe QW creates quite an interesting situation as regards the effect of their interaction on various transport phenomena. In particular, one would expect the effect of binary collisions between the quasiparticles of different type. According to the Pauli exclusion principle only the carriers in the energy interval of the order of kT around the Fermi energy may participate in such collisions, which would supposedly result in a T^2 scaling of resistivity. It has been previously found, that the resistance of a single component system is unaffected by the binary collisions, unless Umclapp processes, involving the presence of the reciprocal lattice vector in the momentum conservation equation, are allowed. This is due to the fact that in a single component system all carriers have the same effective mass and the momentum conservation automatically implies the conservation of the total current. However, if carriers of more than one type are present in the system, than the momentum conservation in the acts of binary scattering involving particles of different types no longer ensures conservation of electrical current. In this case the resistance should become sensitive to binary collisions between particles of different type. The expected experimental evidence of such sensitivity is the T^2 scaling

of resistivity which has been observed for the first time in a 2D semimetal (electron-hole system) on the basis of a HgTe QW [4, 5]. The experimental data has been successfully described by a theory [4, 5] where the binary collisions were included in the form of an interparticle friction coefficient proportional to T^2.

Recently, the 2D electron-hole system in a HgTe QW has also become an object of study in a thermopower experiment in a zero magnetic field, [6]. Comparison between theory and experiment has revealed that the thermo emf in a 2D electron-hole system is determined by two contributions: the diffusion and the phonon drag, with the second contribution several times larger than the first. Conclusions have been drawn about the important role of electron-hole scattering in the formation of both thermoelectric power mechanisms.

The present work continues the study of thermopower phenomena in a 2D electron-hole system based on a HgTe quantum well, but this time in the presence of classically strong magnetic fields. A corresponding theory has been developed taking into account the interparticle scattering that plays an important role in the two principal contributions to the thermopower — the diffusion and the phonon drag. As in the $B = 0$ case, the latter mechanism of thermopower is experimentally found to prevail over the first one.

2. Samples and experimental setup

The investigated samples were fabricated on the basis of a 20 nm wide HgTe quantum well with the orientation (013) previously shown to be a 2D semimetal, Fig. 1. The original wafer containing the HgTe quantum well was patterned into experimental samples of rectangular shape 4×3 mm bearing on top an ordinary Hall structure with $L \times W = 100 \times 50$ μm and 250×50 μm segments between the

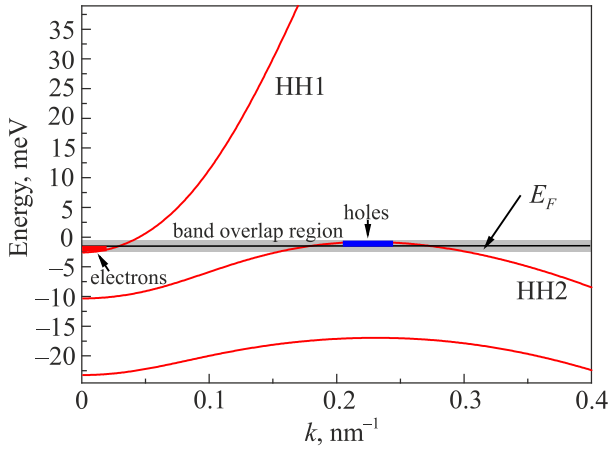

Fig. 1. The calculated energy spectrum of (013) 21 nm wide HgTe quantum well. The shaded area shows the conductance and the valence bands overlap region. The indicated Fermi level position in this area corresponds to a simultaneous presence of electron and holes in the system.

voltage probes prepared by photolithography and chemical etching. The thermoelectric power was measured as follows. At one end of the sample, close to one of the Hall bar current contacts there was a heater, a thin metal strip with a resistance ≈ 50 Ω. The opposite cold end of the sample was indium soldered to a copper piece 5 mm^3, which, in turn, was brought in thermal contact with the massive copper sample holder. To create a temperature gradient along the Hall bar, an alternating current not exceeding 60 mA and with the frequency of 0.4–1 Hz was passed through the heater. For the current range specified, the heater functioned in a linear regime.

To control the gradient along the sample two calibrated thermistors were used — one located at the heater end and the other at the cold end of the sample. For example, the temperature difference thus determined between the voltage contacts 100 μm apart at the ambient temperature $T = 4.2$ K and the heater voltage $V_{p-p} = 6$ V was $\Delta T \approx 0.023$ K or, equivalently, $\nabla T = 230$ K/m. In the operating temperature range (≈ 2.2–4.2 K) the thermal conductivity of liquid helium is negligible compared to phonon thermal conductivity of the wafer substrate. In these conditions, it is the thermal conductivity of the substrate that determines the temperature gradient along the sample. The thermopower signal was measured at a double frequency using available voltage contacts. Experimentally measured quantities were the longitudinal thermovoltage $V_{xx} = S_{xx} \nabla T \cdot L$, where $L = 450$ or 100 μm is the distance between the voltage probes along the temperature gradient ∇T, and the transverse thermovoltage $V_{xy} = S_{xy} \nabla T \cdot W$, where $W = 50$ μm is the sample width normal to the temperature gradient. From V_{xx} and V_{xy} thus obtained the Seebeck S_{xx} and the Nernst S_{xy} coefficients could be evaluated for comparison with theory.

The samples were supplied with a Ti/Au metallic top gate, using which the Fermi level could be swept across the energy bands, including the region of the conduction and the valence bands overlap. About a dozen samples have been investigated. Figure 2(a) shows the typical resistivity versus gate voltage dependence in our samples. As one can see, on sweeping the gate voltage bias from positive to negative the resistivity increases from its low value in the conduction band, reaches the maximum at the charge neutrality point (the Fermi level is then situated in the conduction and valence bands overlap region) and then decreases, as the Fermi level moves deeper into the valence band. To compare the experiment with theory the knowledge is required of such parameters as electron density $n_e(V_g)$, hole density $n_h(V_g)$, electron mobility $\mu_e(V_g)$, hole mobility $\mu_h(V_g)$ and $\Theta(V_g)$ — the coefficient characterizing the strength of the electron-hole friction. They can be determined from fitting the two-component Drude model to low field classical magnetoresistance dependences of $\rho_{xx}(B)$ and $\rho_{xy}(B)$. Θ is found by fitting the experimental $R(T)$ dependence in the region of the bands overlap to the theoretical model that takes into account the friction between holes and electrons [4, 5].

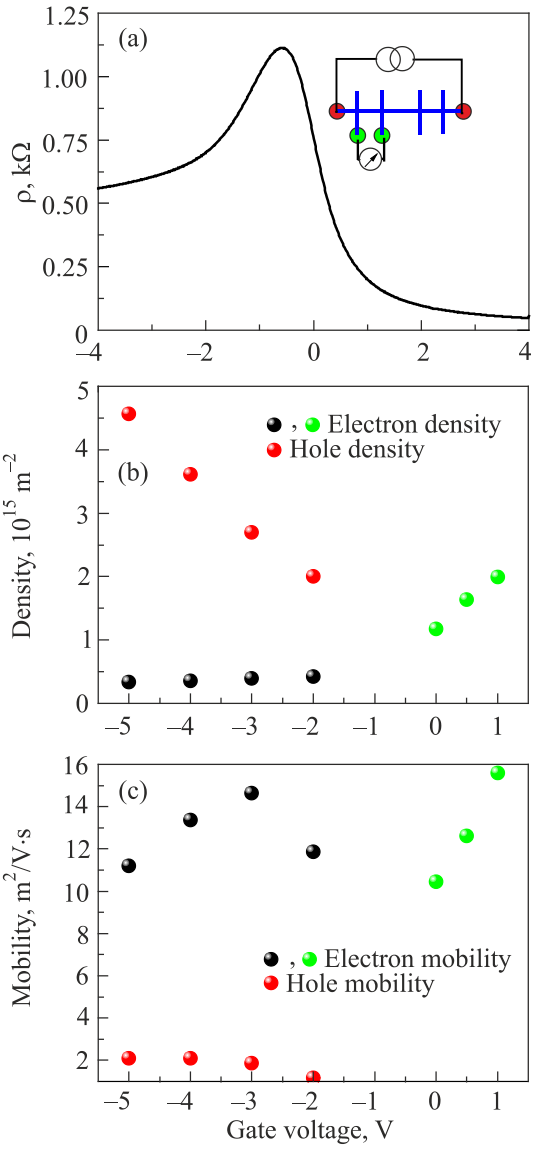

Fig. 2. (Color online) (a) Typical resistivity versus V_g dependence at zero magnetic field and $T = 4.2$ K. The position of the curve's maximum at approximately $V_g = -0.75$ V corresponds to the charge neutrality point — the equality of the electron and hole densities in the quantum well; (b) electron and hole density; (c) electron and hole mobility versus gate voltage. The parameters were determined from fitting the two-component Drude model to low field classical magnetoresistance dependences of $\rho_{xx}(B)$ and $\rho_{xy}(B)$.

The parameters found in this way are summarized in Figs. 2(b) and 2(c), from which the following conclusions can be made:

1) The semimetallic state begins at $V_g \approx 0$.

2) At the charge neutrality point (CNP) $P_s = N_s \approx 10^{11}$.

3) The conduction and valence bands overlap region is about 10 meV in agreement with earlier studies of HgTe 20 nm QWs [3, 4].

4) For all negative biases in Fig. 2(a) the Fermi level never completely quits the conduction band being pinned there by a very high hole density of states in the valence band. It is necessary to note that the bands overlap is several times larger than shown in Fig. 1. Probably this is due to the fact that the strain present in the QW was neglected in the calculations shown in Fig. 1.

3. Results and discussion

3.1. Experimental results

Figure 3 shows the Seebeck coefficient versus gate voltage dependence of the described samples measured at zero magnetic field and $T = 4.2$ K. One can see that at positive gate voltages corresponding to the 2D electron metal state it is negative, relatively small and decreases with electron density increasing according to the Mott expression. In the vicinity of the CNP the Seebeck coefficient changes sign and for negative gate voltages, as the Fermi level moves deeper into the bands overlap region, (i.e., with the hole density increasing and the electron density decreaesing) it grows strongly up to values almost an order of magnitude higher than those at positive biases. So the zero magnetic field Seebeck coefficient behavior in the samples studied is qualitatively the same as reported earlier in [6]. The main part of this paper is devoted to the thermopower behavior in a semimetal state in the presence of magnetic field. As has been shown in [6] the thermopower response in a 2D semimetal is mostly due to the phonon drag contribution which is much larger than the diffusive one.

Figure 4 shows experimentally determined Seebeck tensor coefficients S_{xx} and S_{xy} at $T = 4.2$ K as functions of magnetic field for several values of gate voltage. The gate voltages $V_g = -4, -3, -2$ V correspond to a simultaneous presence of electron and holes in the quantum well [higher negative gate voltage values correspond to lower electron density and higher hole density see Fig. 2(b)].

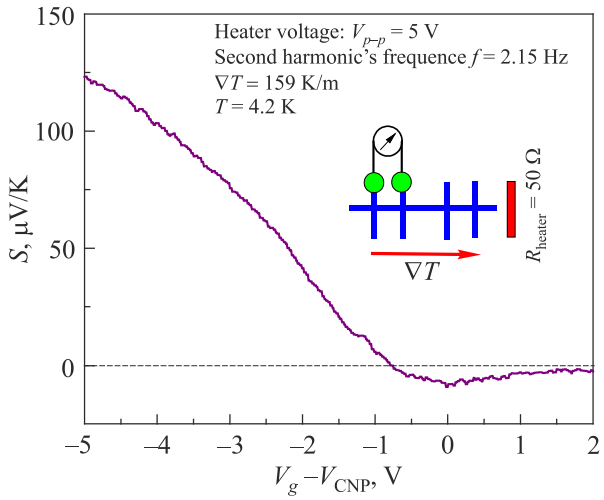

Fig. 3. The thermo emf voltage measured as a function of gate voltage at $B = 0$. Inserts show the experimental setup.

As can be seen from Fig. 4(a) the Seebeck coefficient S_{xx} is symmetric in B, gradually increasing with a tendency to saturation toward $|B| \approx 0.5$ where it is three to four times greater than the corresponding zero field value. The Nernst coefficient S_{xy} Fig. 4(b) is antisymmetric, crossing zero at $B = 0$. The absence of exact antisymmetric graph in the case of S_{xy} in Fig. 4(b) is probably related to the presence of some parasitic pickup. On the whole the experimental S_{xy} curves show some indication of the presence of a maximum at $|B| \approx 0.2$ T. Also, when the Fermi energy is located in the conductance and valence bands overlap region (gate voltages V_g = –4, –3, –2 V), the thermo emf, the overall signal amplitude $S(B) - S(B = 0)$ (both S_{xx} and S_{xy}) increases when the negative gate voltage bias is reduced and one approaches the charge neutrality point, where the hole and electron densities are equal. On the whole, as expected, the described $S_{xx}(B)$ and $S_{xy}(B)$ dependencies are similar to those of $\rho_{xx}(B)$ and $\rho_{xy}(B)$ (not shown).

The experimental results in Figs. 4(a) and 4(b) have been analysed using the theory that takes into account the presence

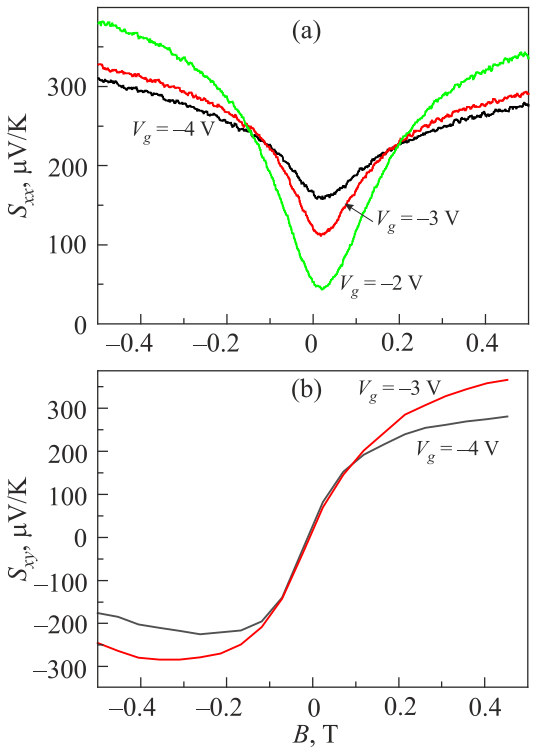

Fig. 4. (a) Seebeck coefficient of a 2D electron-hole system as a function of magnetic field for several values of the gate voltage: $S_{xx}(B) = V_{xx} / (L \cdot \nabla T)$ measured at T = 4.2 K from source-drain probes 450 μm apart (L) and for the temperature gradient along the sample ∇T = 159 K/m (the heater voltage V_{p-p} = 5 V, the second harmonic frequency f = 2.15 Hz). Solid lines — experiment. (b) Nernst coefficient of a 2D electron-hole system as a function of magnetic field for several values of the gate voltage: $S_{xy}(B) = V_{xy} / (W \cdot \nabla T)$ measured at T = 4.2 K from opposite Hall probes 50 μm apart (W) and for the temperature gradient along the sample ∇T = 230 K/m (the heater voltage V_{p-p} = 6 V, the second harmonic frequency f = 1.75 Hz). Solid lines — experiment.

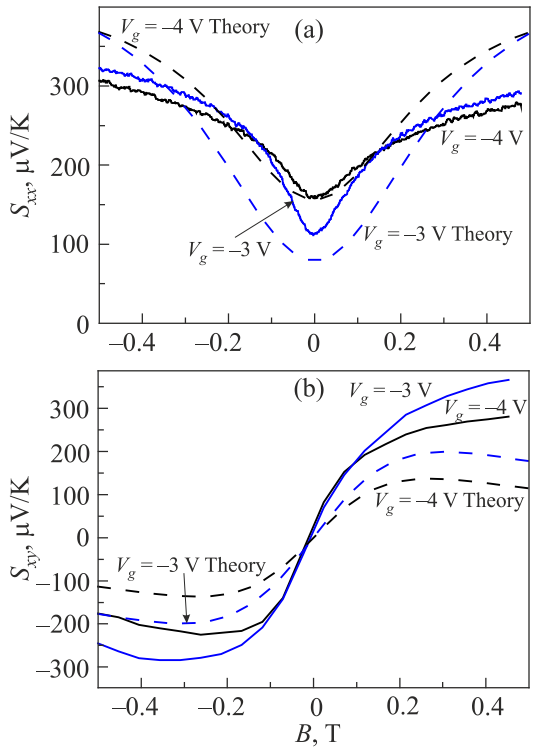

Fig. 5. (a) Seebeck coefficient of a 2D electron-hole system as a function of magnetic field for V_g = –4, – 3 V: solid lines — experiment (see Fig. 4(a) for details); dashed line — calculation for sample parameters corresponding to V_g = –4, – 3 V; (b) Nernst coefficient of a 2D electron-hole system as a function of magnetic field for V_g = –4, – 3 V: solid lines — experiment (see Fig. 4(b) for details); dashed line — calculation for sample parameters corresponding to V_g = –4, – 3 V.

of two different types of charge carriers of opposite sign and their mutual scattering [7]. The theory covers both contributions to the thermo emf — the diffusion and the phonon drag. Supposing that ∇T is directed along axis x, the thermo emf can be written as follows: $E_i = S_{ix}\partial_x T$ $(i = x, y)$. Then, in the case of a strongly degenerate 2D electron-hole system and in the presence of magnetic field the following general expression is obtained for the thermo emf coefficients S_{xy} and S_{xx}:

$$S_{xx} = \frac{\Lambda_x}{Z}, \quad S_{yx} = \frac{\Lambda_y}{Z}, \tag{1}$$

$$Z = (m_e n_h \tau_h + m_h n_e \tau_e + (n_e - n_h)^2 \eta \tau_e \tau_h)^2 + (n_e - n_h)^2 \tau_e^2 \tau_h^2 (eB)^2, \tag{2}$$

$$\Lambda_x = \frac{1}{e}\{[A^e \tau_e m_h - A^h \tau_h m_e + (A^e + A^h)(n_e - n_h)\eta\tau_e\tau_h] + [m_h \tau_e n_e + m_e \tau_h n_h + (n_e - n_h)^2 \eta \tau_e \tau_h] + (A^e + A^h)(n_e - n_h)\tau_e^2 \tau_h^2 (eB)^2\}, \tag{3}$$

$$\Lambda_y = \tau_e \tau_h (A^e n_h + A^h n_e)(m_h \tau_e + m_e \tau_h) B, \tag{4}$$

where $A^{\nu} = A^{\nu}_{\text{dif}} + A^{\nu}_{\text{ph–dr}}$ $(\nu = e, h)$ are the electrons and holes related quantities corresponding to the diffusion and phonon-grag contributions to the thermo emf respectively, n_e and n_h are the electron and hole densities, $m_e = 0.025m_0$ and $m_h = 0.15m_0$ — the electron and hole effective mass, $g_e = 1$ and $g_h = 2$ — the electron and hole valley degeneracy, $\tau_e = \dfrac{\mu_e m_e}{e}$ and $\tau_h = \dfrac{\mu_h m_h}{e}$ — the electron and hole transport scattering time, deduced from the electron and hole mobilities respectively, $\omega_e = -\dfrac{eB}{m_e}$ and $\omega_h = \dfrac{eB}{m_h}$ — electron and hole cyclotron frequency, k — Boltzmann constant, $\eta = \Theta \cdot T^2$ — is the electron-hole friction coefficient, proportional to T^2.

The diffusion contribution is given without any adjustable parameters by:

$$A^{\nu}_{\text{dif}} = -\frac{\pi}{3\hbar^2} k^2 T m_{\nu} g_{\nu}. \tag{5}$$

The phonon drag contribution depends on the material specific phonon relaxation rate. If we suppose that τ_{ph} = const, then for temperatures $T \gg sp_F$ (s — the sound velocity, p_F — the Fermi momentum and we also mean that $s \ll v_F$) we obtain:

$$A^{\nu}_{\text{ph–dr}} = -\frac{1}{3\hbar^2} k^2 \tau_{\text{ph}} m_{\nu}^2 s p_{F\nu}^2 g_{\nu} B_{\nu}(q_T), \tag{6}$$

where $q_T = kT/s$ is the thermal phonon vawe vector and for acoustic phonons in cubic crystals the function $B_{\nu}(q)$ reads:

$$B_{\nu}(q) = \frac{\Lambda_{\nu}^2 q}{2\rho s}, \tag{7}$$

here Λ_{ν} are the deformation potential constants, ρ is the crystal density. We also used the literature data for the deformation potential: $\Lambda_e = -4.6$ eV [8] and $\Lambda_h = -0.92$ eV [9]; for ρ and s we have: $\rho = 8.2$ g/cm^3, $s = 3.2 \cdot 10^5$ cm/s.

The diffusion associated $S_{xx}(B)$ and $S_{xy}(B)$ were calculated according Eqs. (1)–(5) for the sample parameters, determined from magnetotransport data, corresponding to the semimetal state (see Fig. 2). No adjustable parameters have been used in the calculation of the diffusive thermo emf. The phonon drag contribution was calculated according Eqs. (1)–(4), (6) using a constant phonon relaxation length $l_{\text{ph}} = 0.06$ cm, determined from the thermo emf temperature dependence in zero magnetic field. This is the evidence that the phonon relaxation length is determined by their scattering on the substrate boundaries. It was found that although the calculated diffusive $S_{xx}(B)$ and $S_{xy}(B)$ dependencies are qualitatively quite similar to the corresponding experimental ones [Figs. 4(a) and 4(b)], yet they are almost an order of magnitude lower in amplitude. The discrepancy observed between the calculated diffusive thermo emf and the experimental curves in Figs. 4(a) and 4(b) shows that in our system the main contribution to the thermo emf comes from the phonon drag. Figs. 5(a) and 5(b) show the comparison between the experimental data for V_g = –4, –3 V and the result of calculation that is the sum of the diffusive and the phonon-drag contributions to the thermo emf. As can be seen a good qualitative and to some extent quantitative agreement is observed between theory and experiment.

Conclusions

In conclusion, this work is the first to study the behavior of the thermo emf of a two-dimensional semimetal in an HgTe quantum well in the presence of a transverse magnetic field. Experimental magnetic field dependences of the Seebeck and Nernst coefficients are obtained at different gate voltages. The obtained experimental dependences are compared with a theory, in which the behavior of the corresponding transport coefficients is explained taking into account the mutual friction of two groups of carriers of opposite sign, present in the quantum well. It is shown that the calculated values of the transport coefficients corresponding to the diffusion contribution are approximately an order of magnitude smaller than those obtained in the experiment. Thus, the thermo emf of the two-dimensional semimetal in the HgTe quantum well is determined mainly by the contribution from the phonon drag. Taking this contribution into account made it possible to determine the phonon relaxation length, which turned out to be temperature independent and caused by phonon scattering at the structure boundaries.

The financial support of this work by Russian Science Foundation (Grant N16-12-10041-P) is acknowledged.

1. M. Z. Hasan and C. L. Kane, *Rev. Mod. Phys*. **82**, 3045 (2010).
2. Xiao-Liang Q and Shou-Cheng Zhang, *Rev. Mod. Phys*. **83**, 345 (2011).
3. Z. D. Kvon, E. B. Olshanetsky, D. A. Kozlov, N. N. Mikhailov, and S. A. Dvoretskii, *JETP Lett.* **87**, 502 (2008).
4. E. B. Olshanetsky, Z. D. Kvon, M. V. Entin, L. I. Magarill, N. N. Mikhailov, and S. A. Dvoretsky, *JETP Lett.* **89**, 290 (2009).
5. M. V. Entin, L. I. Magarill, E. B. Olshanetsky, Z. D. Kvon, N. N. Mikhailov, and S. A. Dvoretsky, *JETP* **117**, 933 (2013).
6. G. M. Gusev, E. B. Olshanetsky, Z. D. Kvon, L. I. Magarill, M. V. Entin, A. Levin, and N. N. Mikhailov, *JETP Lett*. **107**, 789 (2018).
7. M. V. Entin and L. I. Magarill, to be published.
8. C. G. Van der Walle, *Phys. Rev. B* **39**, 1871 (1989).
9. A. Qteiish and R. D. Needs, *Phys. Rev. B* **45**, 1317 (1992).

Термоелектрорушійна сила у двовимірній електронно-дірковій системі у квантових ямах HgTe у присутності магнітного поля. Роль дифузійного та фононного внесків

E. B. Olshanetsky, Z. D. Kvon, G. M. Gusev, M. V. Entin, L. I. Magarill, N. N. Mikhailov

Експериментально досліджено термоелектрорушійну силу двовимірної електронно-діркової системи у квантовій ямі HgTe (21 нм) у присутності магнітного поля. Повідомлено про перше експериментальне спостереження ефекту Нернста–Еттінгсгаузена у двовимірному напівметалі. Порівняння теорії та експерименту показує, що термоелектрорушійна сила визначається двома внесками: дифузією та фононним захопленням, причому останній внесок у кілька разів перевищує перший. Зроблено висновок щодо важливої ролі електронно-діркового розсіяння у формуванні обох механізмів термоелектрорушійної сили.

Ключові слова: квантова яма, двовимірний напівметал, дифузія, фононне захоплення.